Chapter 8

Severity of bleeding tendency in von Willebrand disease is associated with von Willebrand factor string formation

Jiong-Wei Wang, Bieuwke S. Dragt, Richard J. Dirven, Eveline A.M. Bouwens, Jan Voorberg, Karine M. Valentijn, Pieter H. Reitsma
and Jeroen Eikenboom

To be Submitted

Summary

Background: The phenotype of von Willebrand disease (VWD) Vicenza is unique, but its pathogenesis remains elusive. Two type Vicenza VWD patients, one heterozygous for von Willebrand factor (VWF) mutation p.Arg1205His and the other compound heterozygous for VWF mutations p.Arg1205His and p.Arg924Gln, from the same family showed remarkable differences in bleeding tendency.

Objective: To find the molecular mechanism underlying the disparate bleeding severity in the two patients.

Methods: Storage and secretion of VWF was analyzed in transfected HEK293 cells and in patient-derived blood outgrowth endothelial cells (BOECs). VWF strings were characterized under both static and flow conditions.

Results: VWF mutants p.Arg1205His and p.Arg924Gln were stored normally in (pseudo-) Weibel-Palade bodies (WPB) both in transfected HEK293 cells and in BOECs. Histamine-induced release of VWF propeptide from BOECs of the two VWD patients was reduced to a similar extent. Upon stimulation with histamine, similar quantities of VWF strings were released from BOECs derived from a healthy donor or from the patient heterozygous for p.Arg1205His, whereas the quantity of VWF strings was drastically reduced for BOECs derived from the patient compound heterozygous for p.Arg1205His and p.Arg924Gln. In HEK293 cells, p.Arg1205His led to a significant reduction in total production of VWF, basal and regulated secretion of VWF, and to formation of shorter VWF strings. Similarly, p.Arg924Gln reduced regulated secretion of VWF and resulted in shorter VWF strings.

Conclusions: Synergistic effects of p.Arg1205His and p.Arg924Gln on VWF string formation may contribute to the more severe phenotype in the compound heterozygous patient. Failure of unfolding VWF into strings is a new pathogenic mechanism for VWD that remains undetected by the common diagnostic VWF assays.

Introduction

Von Willebrand factor (VWF) is a large multimeric glycoprotein circulating in blood. VWF is exclusively produced in endothelial cells and megakaryocytes. In endothelial cells VWF is stored as helical tubules within an organelle called Weibel-Palade body (WPB) [1,2]. Upon exocytosis VWF is released from WPB and unfurls into ultra-long strings that bind platelets spontaneously under flow [3-5]. VWF plays a pivotal role in primary hemostasis by recruiting platelets to the site of damaged vessel wall and by mediating platelet-subendothelial matrix interactions. Defects in VWF lead to a mild and common inherited human bleeding disorder, von Willebrand disease (VWD). Type 1 VWD is characterized by a low plasma level of VWF (5-50% of normal level) and by a mild to moderate bleeding tendency [4,6,7]. This subtype of VWD is mostly caused by missense mutations of VWF. Several mechanisms underlying type 1 VWD have been proposed, including reduced protein synthesis, increased retention of VWF in the endoplasmic reticulum (ER), and diminished storage and regulated secretion of VWF [4,8]. A recent study suggested that defective VWF string formation may also contribute to the bleeding tendency in type 1 VWD (**Chapters 6, 7**).

VWF mutation p.Arg1205His has been reported in patients with VWD Vicenza [9,10]. VWD Vicenza is characterized by a low plasma level (<0.20 U/mL) but normal platelet level of VWF, and a proportional decrease of VWF antigen and activity. Occasionally, ultra-large VWF multimers are present in some patients [9,11]. Although VWD Vicenza was classified as type 1 VWD, the pathogenesis of VWD Vicenza remains elusive. So far, accelerated clearance and decreased intracellular production of VWF variant p.Arg1205His has been demonstrated [12-16]. The normal to high response of the patients with p.Arg1205His to desmopressin (DDAVP) suggested normal VWF storage in and release from WPB [17]. Whether the DDAVP-induced elevation of plasma VWF is solely attributable to exocytosis of WPB remains unclear [18]. In addition, whether impaired formation of VWF strings is also involved in VWD Vicenza remains unknown.

Blood outgrowth endothelial cells (BOECs) are authentic endothelial cells that can be derived from human peripheral blood [19,20]. BOECs have been derived from patients and proven useful for the investigation of the pathogenesis of VWD [21] (and **Chapter 6**). In order to increase understanding of the pathogenic mechanisms leading to VWD Vicenza, we studied the formation and exocytosis of WPB in BOECs directly derived from two Vicenza patients: one heterozygous for p.Arg1205His and the other one compound heterozygous for p.Arg1205His and a

presumably benign polymorphism, p.Arg924Gln [21,22]. The pathogenic nature of mutations p.Arg1205His and p.Arg924Gln was also evaluated in HEK293 cells. Furthermore, the properties of VWF strings were characterized both under static and under flow conditions.

Materials and methods

Patients

Two type 1 VWD Vicenza patients from one family were enrolled in this study. One patient was compound heterozygous for VWF mutations p.Arg1205His and p.Arg924Gln; the other patient was heterozygous for p.Arg1205His. Plasma was prepared and tested using the standard procedures for FVIII and VWF parameters, including FVIII:C, VWF:Ag, VWF:RCo, VWF:CB and the VWF multimer profile. The study protocol was approved by the Leiden University Medical Center ethics review board. Informed consent was obtained from all subjects in accordance with the Declaration of Helsinki.

BOECs isolation and culture

BOECs were isolated and cultured as previously described in **Chapter 6**. Briefly, 80 mL venous blood from each subject was collected in citrate acid coated S-Monovette tubes (Nümbrecht, Germany). Buffy coat mononuclear cells were isolated by gradient centrifugation over Ficoll-Paque PLUS (GE Healthcare, Diegem, Belgium) and cultured in EGM-2 (Lonza, Breda, The Netherlands) supplemented with 20% fetal bovine serum, a cocktail of growth factors, 100 U/mL penicillin, 100 µg/mL streptomycin and 250 ng/mL amphotericin (Invitrogen). Cells were used at passages 3 to 8 in all experiments unless stated otherwise.

Plasmid constructs and transfection

Recombinant pCI-neo expression plasmid containing full length cDNAs encoding wild-type human VWF (WT-VWF) has been described previously.[23] Mutations p.Arg1205His (c.3864G>A) and p.Arg924Gln (c.2271G>A) were introduced into pCI-neo WT-VWF plasmid with the QuikChange XL Site-Directed Mutagenesis Kit (Stratagene, La Jolla, CA, USA) using primers 5'-GTGAGGTGGCTGGCCGTCATTTTGCCTCAGGAAAG-3' (forward) and 5'-CTTTCCTGAGGCAAAATGACGGCCAGCCACCTCAC-3' (reverse) for p.Arg1205His; and 5'-GTGAAATGCAAGAAACAGGTCACCATCCTGGTGG-3' (forward) and

5'-CCACCAGGATGGTGACCTGTTTCTTGCATTTCAC-3' (reverse) for p.Arg924Gln. The mutations were verified by sequencing.
HEK293 cells (ATCC, Rockville, USA) were cultured in Minimum Essential Medium α Medium (MEM-α, Sigma-Aldrich, St. Louis, MO, USA) supplemented with 10% fetal calf serum, 2 mM L-glutamine and 50 µg/mL gentamicin (Invitrogen, Carlsbad, CA, USA). Cells were transiently or stably transfected by FuGENE HD transfection reagent (Roche Diagnostics, Mannheim, Germany) as previously described [23].

Immunofluorescent analysis of fixed cells
Confluent monolayer of BOECs were fixed, permeabilized and stained essentially as described in **Chapter 6**. HEK293 cells were fixed for immunochemistry 72 hours after transfection. To visualize VWF strings, confluent BOECs and transfected HEK293 cells were stimulated with 100 µM histamine and phorbol-12-myristate-13-acetate (PMA) (Sigma-Aldrich), respectively. Prior to fixation, cells were stimulated at 37 °C for one hour under static conditions. Monoclonal antibody CLB-RAg35 [24] and polyclonal antibody rabbit anti-human VWF (DAKO) were used to visualize VWF. Monoclonal antibody CD62P (Clone AC1.2, BD Biosciences) was used to visualize P-selectin. Polyclonal antibody rabbit anti-human Protein Disulfide Isomerase (PDI) antibody A66 (obtained from Prof. I. Braakman, Department of Chemistry, Utrecht University, Utrecht, The Netherlands) and polyclonal antibody rabbit anti-human β-catenin (Santa Cruz Biotechnology, Santa Cruz, CA, USA) were used to visualize PDI (the ER marker) and β-catenin, respectively. Alexa 488- and Alexa 594-conjugated secondary antibodies were purchased from Invitrogen. Samples were embedded by Aqua-Poly/Mount medium (Polysciences, GmbH, Germany) and analyzed by Leica SL confocal laser scanning microscopy with a 63X/1.40 NA oil objective (Leica Microsystems).

Live cell imaging of flow experiments
Washed platelets were prepared as described in **Chapter 7** and diluted into perfusion medium (50% M199 medium (Invitrogen) and 50% RPMI-1640 medium (Invitrogen) supplemented with 150 mg l-glutamine per 500 ml and 1% pen/strep) at $2.5x10^7$/ml. The flow experiments of HEK293 cells were performed as previously described (**Chapter 7**). Briefly, cells stably expressing VWF variants were cultured in ibiTreat µ-Slide I (Ibidi, Munich, Germany) flow chambers for 24 hours. Cells were stimulated at 37 °C under static conditions for 60 minutes with 160 nM PMA and then perfused with washed platelets at a shear stress of 2.5 dyn/cm^2. Live-cell

imaging was carried out at 37 °C with Leica fluorescence microscopy DMI-6000 at 200X magnification and recorded (3 seconds per video frame) and analyzed with Leica Microsystems LAS-AF6000 software.
To visualize and quantify released VWF strings from stimulated BOECs under flow, BOECs from a T75 tissue culture flask were resuspended in 6 ml of culture medium and seeded in collagen type 1 coated ibidi µ-Slide I 0.4 Luer (Ibidi) and cultured for 5 days. Medium was refreshed daily. Flow experiments were performed at 37 °C with 5% CO_2. Cells were washed with 1 ml of perfusion medium and subsequently perfused with 100 µM histamine for 10 minutes at 2.5 dyn/cm^2. Perfusion medium containing washed platelets ($2.5x10^7$ per ml) and 1/30.000 diluted Alexa 488-labelled rabbit anti-human VWF polyclonal antibody (DAKO) was perfused for 15 minutes. After 5 minutes (between the 5th and 15th minute) images of 10 randomly chosen optical fields were taken using a LSM510 microscope and a plan-neofluor 40X/0.3 oil immersion lens unless stated otherwise (Carl Zeiss, Sliedrecht, the Netherlands). Images were analyzed using ImageJ 1.45s software (Rasband, International Institutes of Health, Bethesde, USA) and Adobe Photoshop CS5.

Statistical analysis
Student's *t*-test was carried out with GraphPad Prism 5.01. $P<0.05$ was considered statistically significant.

Table 1. Characteristics of the two VWD Vicenza patients

Patient	Gender	Blood group	Nucleotide change	Amino acid change	VWF:Ag, IU/dL	VWF:RCo, IU/dL	VWF:RCo/ VWF:Ag	FVIII:C, IU/dL	VWF:CB, IU/dL	Tesetto Bleeding score	Multimer pattern
P6F5II1	Male	O/O	c.3864G>A and c.2271G>A	p.Arg1205His and p.Arg924Gln	11	7	0.64	18	6	18	Normal
P6F5III1	Female	O/O	c.3864G>A	p.Arg1205His	15	17	1.13	28	Not tested	3	Normal

Results

Phenotypic characterization of the patients

The two VWD Vicenza patients are from the same family. The father is compound heterozygous for VWF mutations p.Arg1205His and p.Arg924Gln and the daughter is heterozygous for VWF mutation p.Arg1205His. Both patients have blood group O (Table 1). Based on the low plasma VWF levels, the proportionally low FVIII and VWF activities (Table 1), and the normal VWF multimer patterns (Figure 1), both patients fitted the diagnosis of type 1 VWD [6]. The father (compound heterozygote) was historically diagnosed as type 1 VWD because of severe bleeding episodes with a Tosetto bleeding score of 18 [25], whereas the daughter was almost asymptomatic (Tosetto bleeding score of 3).

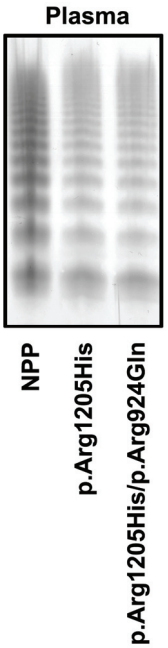

Figure 1. Multimer analysis of plasma VWF. VWF multimers were analyzed by SDS-agarose gel electrophoresis and Western blot under non-reducing conditions. Normal pooled plasma (NPP) was used as reference.

Expression of VWF variants in HEK293 cells

To confirm the pathogenic nature of VWF mutations *per se*, we expressed VWF variants p.Arg1205His and p.Arg924Gln into HEK293 cells. Both variants were stored normally in pseudo-WPB as WT-VWF (Figure 2A-C). No increase in retention of VWF in the ER was observed (Figure 2A-C).

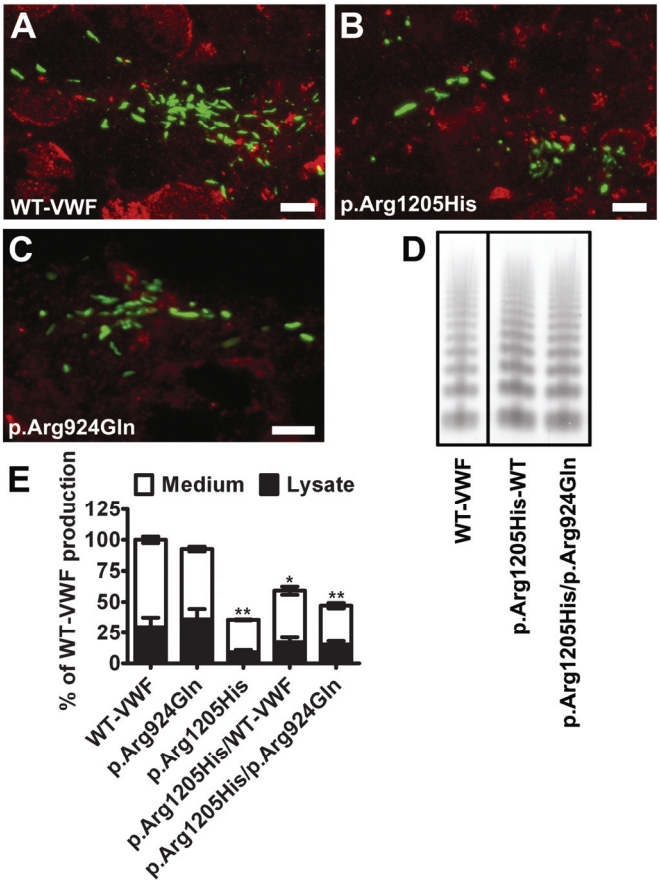

Figure 2. Expression of VWF variants in HEK293 cells. HEK293 cells were transiently transfected with WT-VWF, p.Arg1205His, p.Arg924Gln or a combination as indicated. (A-C) Transfected cells were fixed and stained for VWF and the ER marker PDI, respectively. Scale bars in panels A-C represent 5 µm. Images were taken by Leica SL confocal laser scanning microscopy with a 63X/1.40 NA oil objective. (D) HEK293 cells were transiently transfected with WT-VWF, or co-transfected as indicated at a 1:1 ratio. VWF released into the culture medium was used for multimer analysis. (E) VWF:Ag in the media (Medium) and the cell lysate (Lysate) were measured 72 hours after transfection. VWF in the medium and lysate was expressed as a fraction of total WT-VWF production (medium plus lysate), respectively. Student's t-test compared to WT-VWF *p<0.05, **p<0.01.

In order to mimic the heterozygous and compound heterozygous states in the two VWD Vicenza patients, we co-expressed VWF variant p.Arg1205His with WT-VWF or p.Arg924Gln at a 1:1 ratio. Consistent with the multimer patterns in the plasma from the two patients (Figure 1), there was no alteration in the multimer patterns of

VWF that was secreted into the culture medium (Figure 2D). Furthermore, production and basal secretion of VWF variant p.Arg924Gln was normal compared to WT-VWF (Figure 2E). In contrast, p.Arg1205His reduced the production and basal secretion of VWF by more than 60%. Co-transfection with WT-VWF or p.Arg924Gln corrected this impairment only partially (Figure 2E).

In HEK293 cells VWF is stored in pseudo-WPB that undergo exocytosis upon stimulation just as the authentic WPB in endothelial cells [23,26]. We induced the exocytosis of pseudo-WPB by PMA and measured the release of VWFpp. As shown in Figure 3, 60% of VWFpp was released from WT-VWF transfected HEK293 cells (146 mU from $7x10^5$ cells in 60 minutes). VWF mutation p.Arg1205His drastically impaired exocytosis of pseudo-WPB (27% of total VWFpp or 18 mU VWFpp from $7x10^5$ cells in 60 minutes). VWF mutation p.Arg924Gln led to a similar defect albeit to a lesser extent. The regulated secretion of VWF mutant p.Arg1205His was partially restored by co-expression of WT-VWF or p.Arg924Gln (Figure 3).

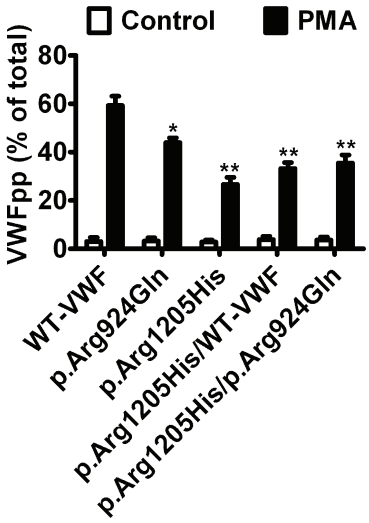

Figure 3. Regulated secretion of VWFpp from transfected HEK293 cells. HEK293 cells were transfected as indicated. Seventy-two hours after transfection cells were stimulated with 160 nM PMA for 60 minutes at 37 °C. VWFpp was measured in the medium and cell lysates. The fraction of secreted VWFpp (% of total) was calculated as described in the Methods. Each bar represents the mean ± SEM of four independent experiments. Student's *t*-test compared to WT-VWF *p<0.05, **p<0.01.

VWF string formation on transfected HEK293 cells

Effects of VWF mutations p.Arg1205His and p.Arg924Gln on the formation of VWF strings were analyzed by transfection of WT-VWF or VWF mutants into HEK293 cells. Upon stimulation with PMA under static conditions, as reported in **Chapter 7**, up to several hundred micrometers long (WT-)VWF strings readily appeared on the surface of HEK293 cells (Figure 4A). Those strings could form bundles and networks. Similar string structures were observed for the cells expressing p.Arg1205His (Figure 4B). VWF mutant p.Arg924Gln primarily gave rise to short VWF strings (Figure 4C-D).

We also generated stable HEK 293 cell lines expressing WT-VWF or VWF variant p.Arg1205His. Upon perfusion of platelets over PMA-stimulated HEK293 cells at a shear stress of 2.5 dyn/cm^2, platelet-decorated VWF strings appeared in the direction of flow for both cell lines (data not shown). Interestingly, the majority of the platelet-decorated VWF strings generated from p.Arg1205His expressing HEK293 cells were significantly shorter than those derived from WT-VWF expressing cells (Figure 5). Whether VWF mutation p.Arg924Gln led to shorter platelet-decorated VWF strings needs further investigation.

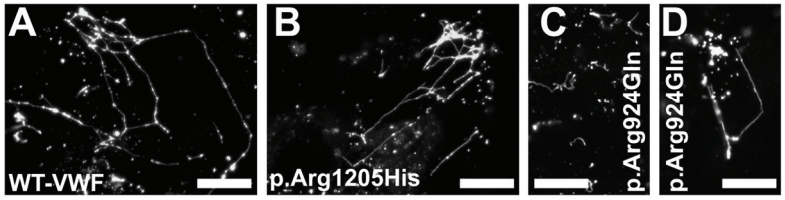

Figure 4. Formation of VWF strings under static conditions on transfected HEK293 cells. HEK293 cells transiently transfected with WT-VWF (A), p.Arg1205His (B) or p.Arg924Gln (C and D) were stimulated with 160 nM PMA for 60 minutes at 37 °C. Cells were fixed and stained for VWF to label VWF strings. Scale bars represent 10 µm. Images were taken by Leica SL confocal laser scanning microscopy with a 63X/1.40 NA oil objective.

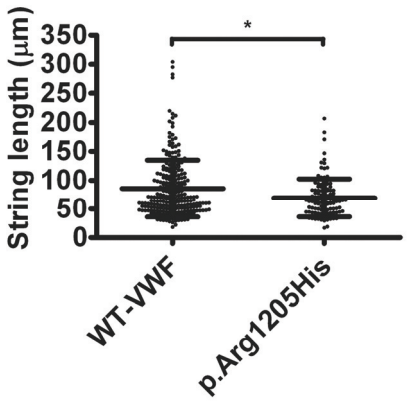

Figure 5. Length of platelet-decorated VWF strings formed on transfected HEK293 cells. HEK293 cells stably expressing WT-VWF or p.Arg1205His were stimulated with PMA for 60 minutes. Thereafter washed platelets were perfused over the cells at a shear stress of 2.5 dyn/cm^2. Images were taken with a Leica DMI-6000 fluorescence microscope at 200X magnification and analyzed with Leica Microsystems LAS-AF6000 software. VWF strings generated from four independent experiments were plotted. Mean ± SD was presented. *p<0.01.

Storage and secretion of VWF revealed by BOECs

We isolated BOECs from a healthy donor and two Vicenza patients. As described in **Chapter 6**, BOECs are authentic endothelial cells that express CD31 (not shown) and store both VWF and P-selectin in WPB (Figure 6A). Immunofluorescence analysis showed that normal WPB were formed both in BOECs derived from the healthy donor and in BOECs derived from the two VWD patients (Figure 6B-C). In addition, VWF secreted from BOECs derived from all the three subjects showed an identical multimer pattern (Figure 6D).

Since endothelial WPB serve as the main source of plasma VWF, we examined the regulated secretion of VWFpp to assess the function of WPB in BOECs. Upon stimulation with 100 μM histamine for 60 minutes, release of VWFpp from all three BOECs lines increased significantly over non-stimulated control cells (Figure 6E). About 70% of VWFpp was secreted from BOECs derived from the healthy donor, while about 40% of VWFpp was secreted from BOECs derived from the two patients (Figure 6E). The absolute amount of VWFpp secreted into the release medium was also reduced for BOECs derived from the two VWD patients (382 mU for healthy BOECs versus 93~94 mU for BOECs derived from the two patients; secreted by 10^5 cells in 60 minutes). No significant difference in VWFpp secretion between BOECs from the two patients was evidence.

Properties of VWF strings derived from BOECs

VWF strings released from BOECs were first analyzed under static conditions. Upon stimulation with histamine, VWF strings were readily visible on the cell surface of BOECs from the healthy donor (Figure 7A). Similar strings were

observed for BOECs heterozygous for p.Arg1205His (Figure 7B), while only few and short strings appeared on the cell surface of BOECs compound heterozygous for p.Arg1205His and p.Arg924Gln (Figure 7C).

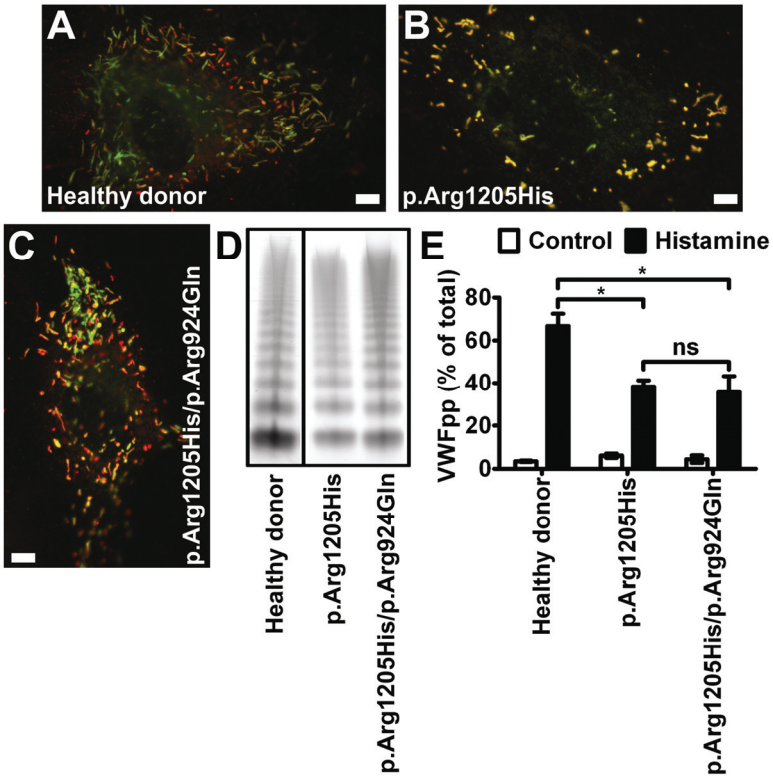

Figure 6. VWF storage in and secretion from BOECs. (A-C) BOECs derived from the healthy donor, from the patient heterozygous for VWF mutation p.Arg1205His or from the patient compound heterozygous for VWF mutations p.Arg1205His and p.Arg924Gln were fixed and stained for VWF and P-selectin. The co-localization of P-selectin and VWF (shown in yellow) indicates storage of P-selectin in WPB. Scale bars represent 5 µm. Images were taken by Leica SL confocal laser scanning microscopy with a 63X/1.40 NA oil objective. (D) VWF multimers in the culture medium of BOECs were analyzed by SDS-agarose gel electrophoresis and Western blotting under non-reducing conditions. The lanes separated by the black lines are from different parts of one gel. (E) Regulated secretion of VWFpp from BOECs. Confluent BOECs derived from the healthy donor and the two patients were incubated for 60 minutes at 37 °C with the release medium in the absence (Control) or presence of 100 µM histamine (Histamine). VWFpp was measured in the medium and lysates. The fraction of secreted VWFpp (% of total) was calculated as described in the Methods. Mean ± S.D. indicates variation of VWFpp secretion between three passages. *p<0.01; ns: the difference is statistically not significant.

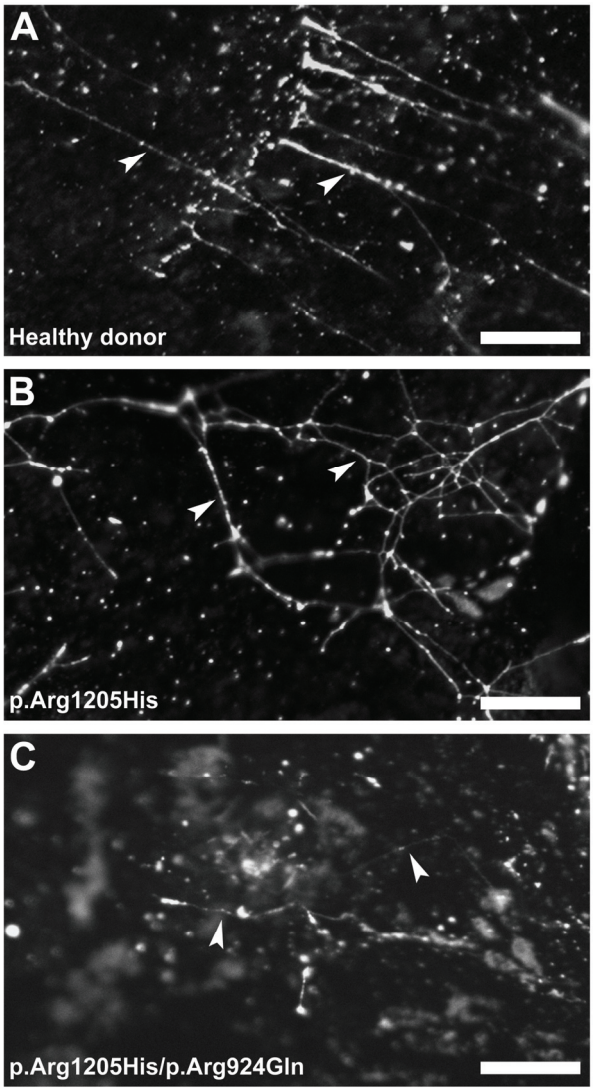

Figure 7. Formation of VWF strings on BOECs under static conditions. BOECs derived from the healthy donor (A) and the two patients (B, C) were cultured on pre-coated coverslips until confluent. Cells were stimulated under static conditions at 37 °C for 60 minutes with 100 µM histamine and then fixed and stained for VWF to visualize VWF string structures. VWF strings are indicated by the arrowheads. Scale bars represent 10 µm. Images were taken by Leica SL confocal laser scanning microscopy with a 63X/1.40 NA oil objective.

To characterize the properties of the VWF strings under physiological conditions, platelets were perfused over histamine-stimulated BOECs under a shear stress of 2.5 dyn/cm^2. Meanwhile VWF strings were also stained with an Alexa-488 labeled VWF antibody. As shown in Figure 8A, both platelet-decorated and platelet-bare VWF strings appeared under flow. To quantify VWF strings, images were taken from 10 random fields in each experiment (Figure 8B and Figure S1). Approximately 30 VWF strings (total of platelet-bound and -bare strings) per 10 fields were observed for BOECs derived from the healthy donor and from the heterozygous patient (Figure 9). Under the same experimental conditions, BOECs derived from the compound heterozygous patient released a smaller number of VWF strings. Actually, in two of the four independent experiments, no strings were observed at all for BOECs derived from the compound heterozygous patient (supplemental Figure S1). Instead, abundant extracellular VWF "patches" appeared on the cell surface of BOECs derived from this patient (Figure 8, right panel). Of the VWF strings derived from the healthy BOECs and BOECs from the heterozygous patient, approximately 45% bound platelets. A similar percentage of platelet-binding VWF strings were observed for BOECs derived from the compound heterozygous patient in the case that strings were formed (data not shown). Furthermore, the density of platelet binding was slightly reduced for VWF strings released from the two patients' BOECs (0.12 versus 0.15 platelets per µm string for BOECs derived from the healthy donor). The binding properties of VWF strings derived from the compound heterozygous patient were not clear because of the limited number of strings available for analysis.

Discussion

In this study we investigated the pathogenesis of VWD Vicenza by transient transfection of VWF variants into HEK293 cells and by analyzing BOECs derived from two Vicenza patients. We found that VWD Vicenza mutation p.Arg1205His reduced regulated secretion of VWF and impaired formation of VWF strings. In addition, compound heterozygosity of VWF mutation p.Arg924Gln was deleterious for the unfolding of VWF into strings and this may enhance the bleeding tendency in VWD Vicenza.

VWD Vicenza has a unique phenotype: a very low plasma level of VWF, combined with the presence of ultra-large VWF multimers in some patients and a normal level of VWF in platelets [9,11]. So far, several scenarios have been proposed to explain the VWD Vicenza phenotype.

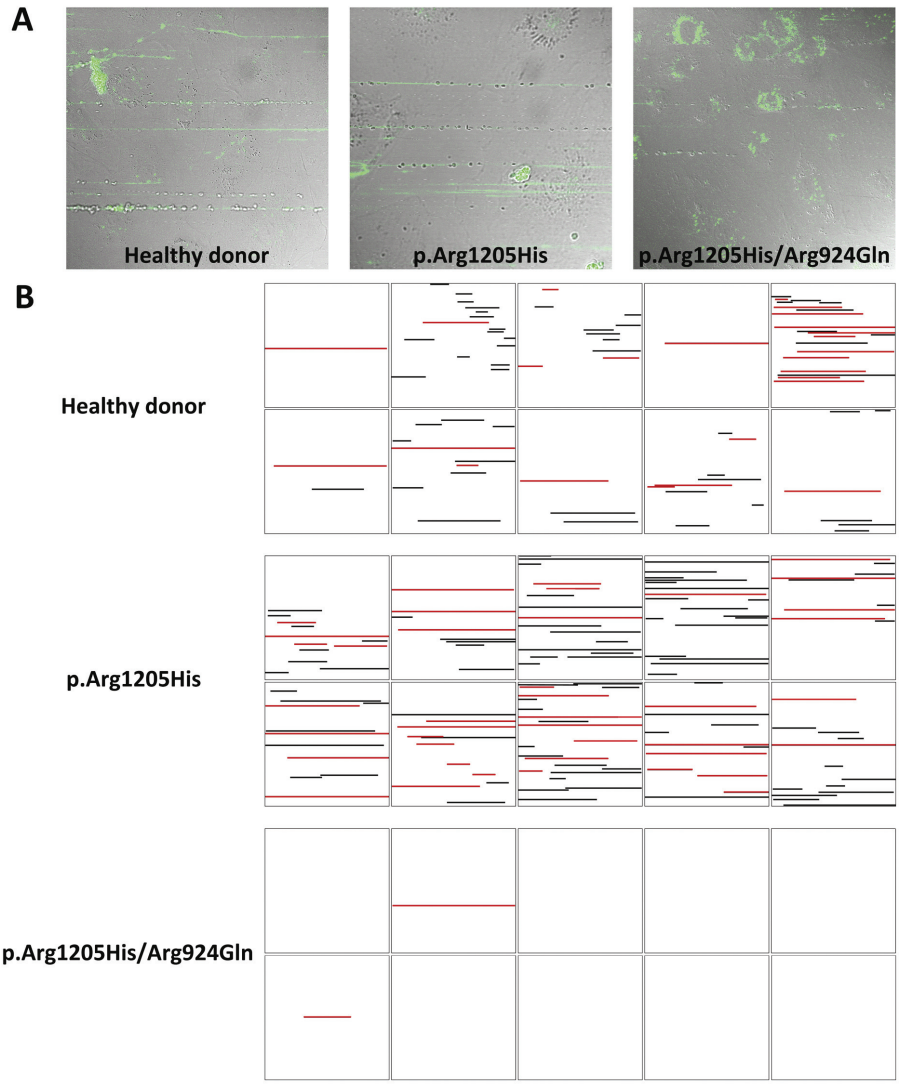

Figure 8. VWF strings released from BOECs under flow. BOECs derived from the healthy donor and the two patients were cultured in collagen-coated flow chambers until confluent. Cells were stimulated under flow of a shear stress at 2.5 dyn/cm^2 at 37 °C for 10 minutes with 100 µM histamine. Thereafter washed platelets and the Alexa-488 labeled VWF antibody were perfused over the cells for 15 minutes. (A) Representative confocal images are shown for VWF strings released from three different BOECs as indicated. Of note, a subset of VWF strings did not bind platelets. (B) VWF strings generated in 10 random imaging fields were transformed into barcodes. The red lines indicate platelet-binding VWF strings and the black lines indicate platelet-bare VWF strings. One representative experiment out of four for each of the BOECs is shown. Images were generated using a LSM510 microscope with a plan-neofluor 40X/0.3 oil immersion lens.

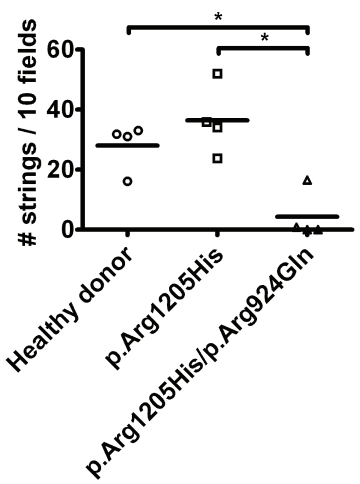

Figure 9. Number of BOECs-derived VWF string under flow. Images generated from figure 8 were analyzed for the number of VWF strings per 10 fields. Each plot represents the total number of VWF strings observed in 10 random fields for each of the BOECs in one experiment. Mean ± S.D. indicates variation within four independent experiments. *p<0.01.

At least two mechanisms have been suggested for the low plasma level of VWF: decreased biosynthesis and accelerated clearance of VWF. Both mechanisms are supported by experimental evidence. Decreased synthesis of VWF mutant p.Arg1205His has been demonstrated in several cell lines for both human and murine VWF [13]. In contrast, this mutation has also been reported not to alter biosynthesis of VWF upon expression in 293T cells [15]. In the current study we showed that the mutation p.Arg1205His did reduce production of VWF in the homozygous, heterozygous and compound heterozygous (with mutation p.Arg924Gln) states in HEK293 cells. The defective effect of p.Arg1205His on total production of VWF was also indicated by the lower amount of total VWFpp antigen in BOECs derived from the two patients than in BOECs derived from the healthy donor (data not shown). Since no apparent retention of VWF mutant p.Arg1205His in the ER occurred, we suspect that the mutation p.Arg1205His more likely led to defective biosynthesis of VWF.

Increased clearance of this VWF mutant has been demonstrated by administration of DDAVP in Vicenza patients and by infusion of recombinant human VWF mutant p.Arg1205His in mice [12,13]. An increased ratio of VWFpp/VWF in the patients [16] and in mice after hydrodynamic expression of this mutant [13] also confirmed the short half-life of VWF mutant p.Arg1205His. Recent evidence showed that faster clearance of VWF is not a unique mechanism for p.Arg1205His, but also accounted for the reduced plasma levels of other type 1 VWD variants [16,27,28].

Even though the macrophage has been suggested to be involved in the clearance of VWF [28,29], the molecular mechanisms that explain why some VWF mutants are cleared faster than others remain elusive.

In order to explain the reduced VWF level and the presence of ultra-large VWF multimers in plasma of VWD Vicenza patients, Gezsi et al developed a mathematical model that simulated the catabolism of VWF. They found that accelerated clearance alone could explain the unique phenotype of VWD Vicenza [15]. The premise of this model was the normal synthesis and cleavage of VWF. As discussed above, however, the synthesis of VWF p.Arg1205His is actually reduced (Figure 2) [13]. Whether p.Arg1205His alters the cleavage of VWF by ADAMTS-13 is not clear although hydrodynamic expression of VWF in mice showed normal cleavage of VWF mutant p.Arg1205His [13].

Defective storage and regulated secretion of VWF has been shown for several type 1 VWD mutations [23,26,30,31]. We demonstrated that p.Arg1205His reduced the regulated secretion of VWF from pseudo-WPB in HEK293 cells and from BOECs derived from VWD Vicenza patients. In contrast to other type 1 VWD mutations, no obvious retention of VWF in the ER was observed for VWF mutant p.Arg1205His. Therefore, the decrease in regulated secretion of VWF mutant p.Arg1205His probably results from decreased production of VWF. Other undefined factors such as alteration in VWF tubular storage may also contribute to the defect in regulated secretion of VWF/VWFpp.

VWF is stored as highly condensed tubules within WPB. This storage relies on an acidic pH environment and a high concentration of calcium. Upon exposure to neutral pH during exocytosis, VWF is released and unfurled into ultra-long strings of up to several hundred microns [3-5]. VWF strings are assumed to bind platelets spontaneously and thus promote clot formation and tissue repair. Interestingly, not all newly released VWF strings bind platelets [32]. We found that a subgroup (~45% of total) VWF strings released from BOECs bound platelets under a shear stress of 2.5 dyn/cm^2. This is similar to the VWF strings released from HUVECs of which about 33% bind platelets at the same shear stress [32]. The ratio between the platelet-binding and platelet-bare VWF strings was not altered by inheritance of VWF mutations p.Arg1205His and p.Arg924Gln in BOECs derived from the two patients. Furthermore, our preliminary data showed that the binding of platelets under flow was only slightly reduced for VWF strings released from BOECs derived from the two VWD Vicenza patients. Thus the Vicenza mutation has little or no effect on the binding capacity of VWF strings.

The two VWD Vicenza patients have similar VWF plasma levels and multimer patterns (Table 1) and comparable storage and regulated secretion of VWF from BOECs (Figure 6), whereas the patient compound heterozygous for p.Arg1205His and p.Arg924Gln shows a severe bleeding tendency and the patient heterozygous for p.Arg1205His is almost asymptomatic. Apparently the conventional laboratory results (Table 1) do not explain the remarkable differences in the Tosetto bleeding scores of the two patients (18 versus 3). Under both static and flow conditions, BOECs derived from the compound heterozygous patient released much fewer and shorter VWF strings compared with BOECs derived from the heterozygous patient (Figures 7-9 and Figure S1). Detailed analysis demonstrated that the low number of VWF strings resulted from insufficient unfolding of released VWF (indicated by formation of VWF patches seen in Figure 8A, right panel). In addition, both VWF mutations p.Arg924Gln and p.Arg1205His gave rise to shorter VWF strings on transfected HEK293 cells (Figures 4 and 5). On the basis of these findings we postulate that synergistic effects of the two mutations on VWF string formation led to a very low number and shorter length of VWF strings formed on the cell surface of BOECs derived from the compound heterozygous patient. In contrast, the detrimental effect of p.Arg1205His on formation of VWF strings may have been corrected, in part, by the wild type VWF in BOECs derived from the heterozygous patient. Since impairment of the formation and function of VWF strings may decrease the hemostatic activity of VWF, the defective formation of VWF string may explain the severe phenotype of the compound heterozygous patient. This suggests that VWF mutations may well result in similar phenotypic characteristics in routine laboratory tests, including VWF:Ag, VWF:RCo and VWF multimers, but may have a remarkable difference in string formation due to VWF mutations *per se* or other unknown factors.

As discussed above, VWF mutation p.Arg924Gln appeared to add to the severity of p.Arg1205His. The pathogenic effects of VWF mutation p.Arg924Gln have been controversial [22]. p.Arg924Gln was reported as a frequent mutation in three type 1 VWD studies [33-35]. Further study demonstrated that this mutation was associated with low plasma levels of both VWF and FVIII even in the normal populations [36,37]. Despite this, no defects in VWF biosynthesis or intracellular storage were observed in expression studies [21,37]. Consistent with those previous studies, we found that p.Arg924Gln did not alter VWF biosynthesis and its trafficking from the ER into pseudo-WPB in HEK293 cells. The regulated secretion of VWF, however, was reduced by p.Arg924Gln in the present study. This is

different from a previous study in AtT20 cells in which no alteration in the regulated secretion of VWF variant p.Arg924Gln was observed [21]. The difference may be explained by differences between the model systems (HEK293 cells versus AtT20 cells) and by different WPB secretagogues (PMA versus $BaCl_2$). In addition, different assays to estimate regulated secretion of VWF may explain for the differential observations. We measured the release of VWFpp instead of VWF as we found that measuring VWFpp is better for estimating exocytosis from (pseudo-)WPB (**Chapters 6** and **7**). Indeed, upon stimulation the release of VWFpp increased by 11 folds over controls (Figure 3), whereas in the previous report the increase in VWF release was only 1.6 fold [21]. Since p.Arg924Gln is commonly co-inherited with other VWF mutations, its additive effect on the defective formation of VWF strings may explain the variable phenotype in VWD patients carrying this mutation [21,22,35-37].

In conclusion, we demonstrated, in both transfected HEK293 cells and BOECs derived from two Vicenza VWD patients, that p.Arg924Gln and p.Arg1205His impaired the regulated secretion of VWF and the formation of VWF strings. The lack of unfolding of VWF into strings is a new pathogenic mechanism of VWD that cannot be detected by the routine diagnostic VWF assays. Co-inheritance of p.Arg924Gln and p.Arg1205His has additive effects on VWF string formation and consequently on the severity of bleeding tendency in the patients.

Acknowledgements

This work was financially supported by grants from the China Scholarship Council (2007U21083) and the Netherlands Organisation for Scientific Research (NWO, grant no. 91209006).

We would like to thank Dr. Herm-Jan Brinkman from Department of Plasma Proteins, Sanquin-AMC Landsteiner Laboratory (Amsterdam) for arranging VWFpp ELISA kits.

References

1. Wagner DD. Cell biology of von Willebrand factor. *Annu Rev Cell Biol* 1990; **6**:217-246.
2. Sadler JE. Biochemistry and genetics of von Willebrand factor. *Annu Rev Biochem* 1998; **67**:395-424.
3. Dong JF, Moake JL, Nolasco L, Bernardo A, Arceneaux W, Shrimpton CN, Schade AJ, McIntire LV, Fujikawa K, Lopez JA. ADAMTS-13 rapidly cleaves newly secreted ultralarge von Willebrand factor multimers on the endothelial surface under flowing conditions. *Blood* 2002; **100**:4033-4039.

4. Valentijn KM, Sadler JE, Valentijn JA, Voorberg J, Eikenboom J. Functional architecture of Weibel-Palade bodies. *Blood* 2011; **117**:5033-5043.
5. Michaux G, Abbitt KB, Collinson LM, Haberichter SL, Norman KE, Cutler DF. The physiological function of von Willebrand's factor depends on its tubular storage in endothelial Weibel-Palade bodies. *Dev Cell* 2006; **10**:223-232.
6. Sadler JE, Budde U, Eikenboom JC, Favaloro EJ, Hill FG, Holmberg L, Ingerslev J, Lee CA, Lillicrap D, Mannucci PM, Mazurier C, Meyer D, Nichols WL, Nishino M, Peake IR, Rodeghiero F, Schneppenheim R, Ruggeri ZM, Srivastava A, Montgomery RR, Federici AB. Update on the pathophysiology and classification of von Willebrand disease: a report of the Subcommittee on von Willebrand Factor. *J Thromb Haemost* 2006; **4**:2103-2114.
7. Goodeve A. Genetics of type 1 von Willebrand disease. *Curr Opin Hematol* 2007; **14**:444-449.
8. Wang JW, Eikenboom J. Von Willebrand disease and Weibel-Palade bodies. *Hamostaseologie* 2010; **30**:150-155.
9. Schneppenheim R, Federici AB, Budde U, Castaman G, Drewke E, Krey S, Mannucci PM, Riesen G, Rodeghiero F, Zieger B, Zimmermann R. Von Willebrand Disease type 2M "Vicenza" in Italian and German patients: identification of the first candidate mutation (G3864A; R1205H) in 8 families. *Thromb Haemost* 2000; **83**:136-140.
10. Castaman G, Missiaglia E, Federici AB, Schneppenheim R, Rodeghiero F. An additional unique candidate mutation (G2470A; M740I) in the original families with von Willebrand disease type 2 M Vicenza and the G3864A (R1205H) mutation. *Thromb Haemost* 2000; **84**:350-351.
11. Mannucci PM, Lombardi R, Castaman G, Dent JA, Lattuada A, Rodeghiero F, Zimmerman TS. von Willebrand disease "Vicenza" with larger-than-normal (supranormal) von Willebrand factor multimers. *Blood* 1988; **71**:65-70.
12. Lenting PJ, Westein E, Terraube V, Ribba AS, Huizinga EG, Meyer D, de Groot PG, Denis CV. An experimental model to study the in vivo survival of von Willebrand factor. Basic aspects and application to the R1205H mutation. *J Biol Chem* 2004; **279**:12102-12109.
13. Pruss CM, Golder M, Bryant A, Hegadorn CA, Burnett E, Laverty K, Sponagle K, Dhala A, Notley C, Haberichter S, Lillicrap D. Pathologic mechanisms of type 1 VWD mutations R1205H and Y1584C through in vitro and in vivo mouse models. *Blood* 2011; **117**:4358-4366.
14. Casonato A, Pontara E, Sartorello F, Cattini MG, Sartori MT, Padrini R, Girolami A. Reduced von Willebrand factor survival in type Vicenza von Willebrand disease. *Blood* 2002; **99**:180-184.
15. Gezsi A, Budde U, Deak I, Nagy E, Mohl A, Schlammadinger A, Boda Z, Masszi T, Evan SJ, Bodo I. Accelerated clearance alone explains ultralarge multimers in VWD vicenza. *J Thromb Haemost* 2010.
16. Haberichter SL, Castaman G, Budde U, Peake I, Goodeve A, Rodeghiero F, Federici AB, Batlle J, Meyer D, Mazurier C, Goudemand J, Eikenboom J, Schneppenheim R, Ingerslev J, Vorlova Z, Habart D, Holmberg L, Lethagen S, Pasi J, Hill FG, Montgomery RR. Identification of type 1 von Willebrand disease patients with reduced von Willebrand factor survival by assay of the VWF propeptide in the European study: molecular and clinical markers for the diagnosis and management of type 1 VWD (MCMDM-1VWD). *Blood* 2008; **111**:4979-4985.
17. Castaman G, Lethagen S, Federici AB, Tosetto A, Goodeve A, Budde U, Batlle J, Meyer D, Mazurier C, Fressinaud E, Goudemand J, Eikenboom J, Schneppenheim R, Ingerslev J, Vorlova Z, Habart D, Holmberg L, Pasi J, Hill F, Peake I, Rodeghiero F. Response to

desmopressin is influenced by the genotype and phenotype in type 1 von Willebrand disease (VWD): results from the European Study MCMDM-1VWD. *Blood* 2008; **111**:3531-3539.

18. Kaufmann JE, Vischer UM. Cellular mechanisms of the hemostatic effects of desmopressin (DDAVP). *J Thromb Haemost* 2003; **1**:682-689.
19. Lin Y, Weisdorf DJ, Solovey A, Hebbel RP. Origins of circulating endothelial cells and endothelial outgrowth from blood. *J Clin Invest* 2000; **105**:71-77.
20. Bouwens EA, Mourik MJ, van den Biggelaar M, Eikenboom JC, Voorberg J, Valentijn KM, Mertens K. Factor VIII alters tubular organization and functional properties of von Willebrand factor stored in Weibel-Palade bodies. *Blood* 2011; **118**:5947-5956.
21. Berber E, James PD, Hough C, Lillicrap D. An assessment of the pathogenic significance of the R924Q von Willebrand factor substitution. *J Thromb Haemost* 2009; **7**:1672-1679.
22. Lester W, Guilliatt A, Grundy P, Enayat S, Millar C, Hill F, Cumming T, Collins P. Is VWF R924Q a benign polymorphism, a marker of a null allele or a factor VIII-binding defect? The debate continues with results from the UKHCDO VWD study. *Thromb Haemost* 2008; **100**:716-718.
23. Wang JW, Valentijn KM, de Boer HC, Dirven RJ, van Zonneveld AJ, Koster AJ, Voorberg J, Reitsma PH, Eikenboom J. Intracellular storage and regulated secretion of von Willebrand factor in quantitative von Willebrand disease. *J Biol Chem* 2011; **286**:24180-24188.
24. Romani de WT, Rondaij MG, Hordijk PL, Voorberg J, van Mourik JA. Real-time imaging of the dynamics and secretory behavior of Weibel-Palade bodies. *Arterioscler Thromb Vasc Biol* 2003; **23**:755-761.
25. Tosetto A, Rodeghiero F, Castaman G, Goodeve A, Federici AB, Batlle J, Meyer D, Fressinaud E, Mazurier C, Goudemand J, Eikenboom J, Schneppenheim R, Budde U, Ingerslev J, Vorlova Z, Habart D, Holmberg L, Lethagen S, Pasi J, Hill F, Peake I. A quantitative analysis of bleeding symptoms in type 1 von Willebrand disease: results from a multicenter European study (MCMDM-1 VWD). *J Thromb Haemost* 2006; **4**:766-773.
26. Michaux G, Hewlett LJ, Messenger SL, Goodeve AC, Peake IR, Daly ME, Cutler DF. Analysis of intracellular storage and regulated secretion of 3 von Willebrand disease-causing variants of von Willebrand factor. *Blood* 2003; **102**:2452-2458.
27. Schooten CJ, Tjernberg P, Westein E, Terraube V, Castaman G, Mourik JA, Hollestelle MJ, Vos HL, Bertina RM, Berg HM, Eikenboom JC, Lenting PJ, Denis CV. Cysteine-mutations in von Willebrand factor associated with increased clearance. *J Thromb Haemost* 2005; **3**:2228-2237.
28. Denis CV, Christophe OD, Oortwijn BD, Lenting PJ. Clearance of von Willebrand factor. *Thromb Haemost* 2008; **99**:271-278.
29. van Schooten CJ, Shahbazi S, Groot E, Oortwijn BD, van den Berg HM, Denis CV, Lenting PJ. Macrophages contribute to the cellular uptake of von Willebrand factor and factor VIII in vivo. *Blood* 2008; **112**:1704-1712.
30. Wang JW, Groeneveld DJ, Cosemans G, Dirven RJ, Valentijn KM, Voorberg J, Reitsma PH, Eikenboom J. Biogenesis of Weibel-Palade bodies in von Willebrand disease variants with impaired von Willebrand factor intrachain or interchain disulfide bond formation. *Haematologica* 2011; **97**:859-866.
31. Castaman G, Giacomelli SH, Jacobi PM, Obser T, Budde U, Rodeghiero F, Schneppenheim R, Haberichter SL. Reduced von willebrand factor secretion is associated with loss of weibel-palade body formation. *J Thromb Haemost* 2012; **10**:951-958.

32. Huang J, Roth R, Heuser JE, Sadler JE. Integrin alpha(v)beta(3) on human endothelial cells binds von Willebrand factor strings under fluid shear stress. *Blood* 2009; **113**:1589-1597.
33. James PD, Notley C, Hegadorn C, Leggo J, Tuttle A, Tinlin S, Brown C, Andrews C, Labelle A, Chirinian Y, O'Brien L, Othman M, Rivard G, Rapson D, Hough C, Lillicrap D. The mutational spectrum of type 1 von Willebrand disease: Results from a Canadian cohort study. *Blood* 2007; **109**:145-154.
34. Goodeve A, Eikenboom J, Castaman G, Rodeghiero F, Federici AB, Batlle J, Meyer D, Mazurier C, Goudemand J, Schneppenheim R, Budde U, Ingerslev J, Habart D, Vorlova Z, Holmberg L, Lethagen S, Pasi J, Hill F, Hashemi SM, Baronciani L, Hallden C, Guilliatt A, Lester W, Peake I. Phenotype and genotype of a cohort of families historically diagnosed with type 1 von Willebrand disease in the European study, Molecular and Clinical Markers for the Diagnosis and Management of Type 1 von Willebrand Disease (MCMDM-1VWD). *Blood* 2007; **109**:112-121.
35. Cumming A, Grundy P, Keeney S, Lester W, Enayat S, Guilliatt A, Bowen D, Pasi J, Keeling D, Hill F, Bolton-Maggs PH, Hay C, Collins P. An investigation of the von Willebrand factor genotype in UK patients diagnosed to have type 1 von Willebrand disease. *Thromb Haemost* 2006; **96**:630-641.
36. Casais P, Carballo GA, Woods AI, Kempfer AC, Farias CE, Grosso SH, Lazzari MA. R924Q substitution encoded within exon 21 of the von Willebrand factor gene related to mild bleeding phenotype. *Thromb Haemost* 2006; **96**:228-230.
37. Hickson N, Hampshire D, Winship P, Goudemand J, Schneppenheim R, Budde U, Castaman G, Rodeghiero F, Federici AB, James P, Peake I, Eikenboom J, Goodeve A. von Willebrand factor variant p.Arg924Gln marks an allele associated with reduced von Willebrand factor and factor VIII levels. *J Thromb Haemost* 2010; **8**:1986-1993.

Supplemental data

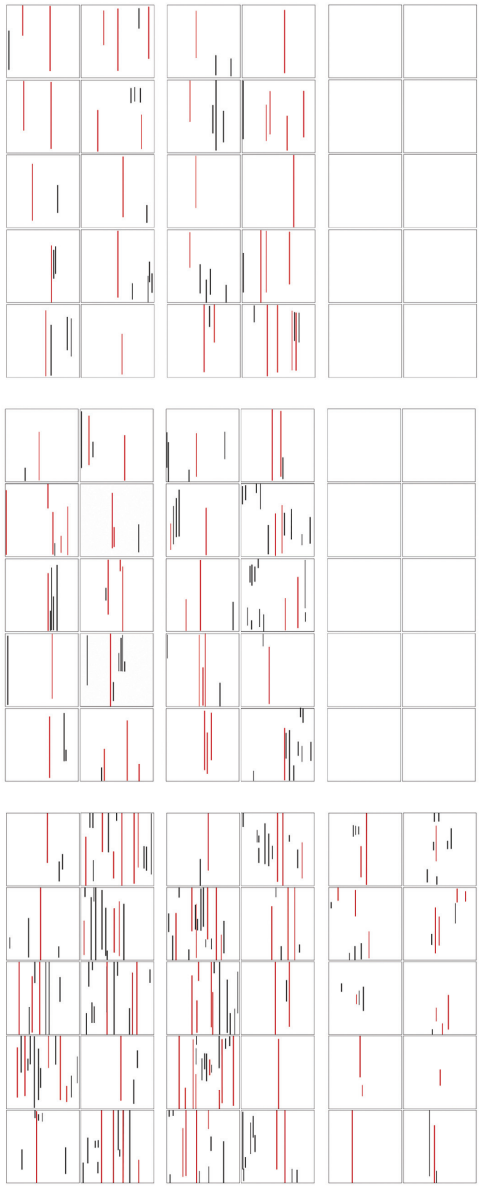

Figure S1. VWF strings released from BOECs under flow. BOECs derived from the healthy donor and the two patients were cultured in collagen-coated flow chambers until confluent. Cells were stimulated under flow of a shear stress at 2.5 dyn/cm2 at 37 °C for 10 minutes with 100 µM histamine. Then washed platelets and the Alexa-488 labeled VWF antibody were perfused over the cells for 15 minutes. VWF strings released from three different BOECs were indicated. Strings generated in 10 random imaging fields for each experiment were transformed into barcodes as in Figure 8. Data from three additional experiments were shown (A-C). The red lines indicate platelet-bound VWF strings and the black lines indicate platelet-bare VWF strings. Images were generated by using a LSM510 microscope with a plan-neofluor 40X (A-B) or 63X/0.3 (C) oil immersion lens.